

# Negative feedback regulation is responsible for the non-linear modulation of photosynthetic activity in plants and cyanobacteria exposed to a dynamic light environment

Ladislav Nedbal<sup>a,\*</sup>, Vítězslav Březina<sup>a</sup>, František Adamec<sup>a</sup>, Dalibor Štys<sup>a</sup>, Vello Oja<sup>b</sup>,  
Agu Laisk<sup>b</sup>, Govindjee<sup>a,c</sup>

<sup>a</sup>Laboratory of Applied Photobiology and Bio-Imaging, Institute of Landscape Ecology CAS and Institute of Physical Biology of University of S. Bohemia, Zámek 136, CZ-37333 Nové Hradky, Czech Republic

<sup>b</sup>Department of Plant Physiology, Institute of Molecular and Cell Biology, University of Tartu, Riia 23, 51010 Tartu, Estonia

<sup>c</sup>Departments of Biochemistry and Plant Biology, University of Illinois, 265 Morrill Hall, 505 S. Goodwin Avenue, Urbana, IL 61801-3707, USA

Received 10 April 2003; received in revised form 28 July 2003; accepted 11 August 2003

## Abstract

Photosynthetic organisms exposed to a dynamic light environment exhibit complex transients of photosynthetic activities that are strongly dependent on the temporal pattern of the incident irradiance. In a harmonically modulated light of intensity  $I \approx \text{const.} + \sin(\omega t)$ , chlorophyll fluorescence response consists of a steady-state component, a component modulated with the angular frequency of the irradiance  $\omega$  and several upper harmonic components ( $2\omega$ ,  $3\omega$  and higher). Our earlier reverse engineering analysis suggests that the non-linear response can be caused by a negative feedback regulation of photosynthesis. Here, we present experimental evidence that the negative feedback regulation of the energetic coupling between phycobilisome and Photosystem II (PSII) in the cyanobacterium *Synechocystis* sp. PCC6803 indeed results in the appearance of upper harmonic modes in the chlorophyll fluorescence emission. Dynamic changes in the coupling of the phycobilisome to PSII are not accompanied by corresponding antiparallel changes in the Photosystem I (PSI) excitation, suggesting a regulation limited to PSII. Strong upper harmonic modes were also found in the kinetics of the non-photochemical quenching (NPQ) of chlorophyll fluorescence, of the P700 redox state and of the CO<sub>2</sub> assimilation in tobacco (*Nicotiana tabacum*) exposed to harmonically modulated light. They are ascribed to negative feedback regulation of the reactions of the Calvin–Benson cycle limiting the photosynthetic electron transport. We propose that the observed non-linear response of photosynthesis may also be relevant in a natural light environment that is modulated, e.g., by ocean waves, moving canopy or by varying cloud cover. Under controlled laboratory conditions, the non-linear photosynthetic response provides a new insight into dynamics of the regulatory processes.

© 2003 Elsevier B.V. All rights reserved.

**Keywords:** Calvin–Benson cycle; Forced oscillation; Intermittent light; Phycobilisome; State transition; Systems analysis

## 1. Introduction

Plants harvest and utilize light energy in a dynamic environment. Due to clouds, sunflecks or, in case of phytoplankton, due to movement in surface waves, incident irradiance can rapidly fluctuate between levels where photosynthesis barely compensates respiration to peaks reaching or exceeding saturation of the photosynthetic reactions [1–4].

In light fluctuations that are faster than the rate-limiting biochemical reactions, the intermittent effects are averaged and the plant is expected to react as if in a steady-state regime characterized by mean values of the environmental parameters. On the other extreme, during very slow changes, the plant has sufficient time to adjust to the environment and its physiology is dominantly controlled by instantaneous irradiance rather than by the conditions during the plant history. Here, we report on the plant response to light fluctuations of an intermediate angular frequency ( $2\pi/5 \text{ min} < \omega < 2\pi/20 \text{ s}$ ) where significant memory effects are expected [5].

Trivial memory effects are caused by finite capacity of metabolite pools (e.g., 3-phosphoglyceric acid, ribulose-1,5-biphosphate, inorganic phosphate, hexosephosphates)

*Abbreviations:* Chl, chlorophyll; PSI, Photosystem I; PSII, Photosystem II; NPQ, non-photochemical quenching; PFD, photon flux density

\* Corresponding author. Tel.: +420-386-361111; fax: +420-386-361231.

E-mail address: nedbal@greentech.cz (L. Nedbal).

that are accumulated or consumed by the preceding photochemical activity. In analogy with water pools of hydrodynamic models, the metabolite pools are expected to oscillate with the frequency of the irradiance, exhibiting a phase shift that depends on the size and turnover rate of the metabolites relative to the frequency of the incident irradiance [6]. More intriguing than the forward filling or drain of the metabolite pools, are coherent memory effects that lead to the autonomous oscillations of photosynthetic responses like, e.g., chlorophyll fluorescence, oxygen evolution or CO<sub>2</sub> assimilation. A simple model representing analogous memory effect is a mechanical spring. If pulled and released, it exhibits autonomous damped oscillations similar to photosynthesis in plants exposed to a sudden change in irradiance or in ambient CO<sub>2</sub> concentration [7–12]. The autonomous photosynthetic oscillations mostly occur with a period close to  $T=2\pi/\omega \approx 60$  s and the oscillation damping is highly variable [9]. By removing the interference of signals from neighboring cells that oscillate at slightly different frequencies, Ferimazova et al. [12] resolved autonomous photosynthetic oscillations of several other characteristic periods and of largely different damping constants indicating that multiple oscillatory mechanisms are present in plants.

In another analogy to a mechanical spring, photosynthetic oscillatory systems can exhibit a resonance response to an external harmonic forcing. Nedbal and Brezina [13] showed recently that the fluorescence response of plants to harmonically modulated irradiance exhibits a resonance peak ( $\omega \approx 2\pi/60$  s) that is related to the dominant autonomous oscillations observed earlier. However, more like a string of a musical instrument than a simple mechanical spring, the chlorophyll (Chl) fluorescence response of a plant to harmonic forcing of a frequency  $\omega$  is shaped by significant upper harmonic components ( $2\omega$ ,  $3\omega$  and higher). The authors [13] proposed that the upper harmonic components in Chl fluorescence originate from a negative feedback regulation of plant photosynthesis. The response of plants to forcing by harmonically modulated light offers a unique insight into the regulatory processes that are of a crucial importance for plants utilizing light energy in a dynamic environment.

Here, we aim at two objectives. First, the earlier proposed causal relationship between regulation and appearance of the upper harmonic modes in fluorescence emission is tested using the known negative feedback regulation of the energetic coupling of phycobilisome antenna to Photosystem II (PSII) in cyanobacteria [14–16]. Second, the ecophysiological relevance of the observed phenomena is investigated in experiments determining not only the kinetics of the forced oscillations in fluorescence emission but also corresponding transients in CO<sub>2</sub> assimilation, non-photochemical quenching (NPQ) of Chl fluorescence and in P700 redox state in intact leaves of tobacco. The appearance of the upper harmonic modes in the CO<sub>2</sub> assimilation reported here proves that the newly found non-linear effect has an impact reaching

beyond the limits of the primary photochemical reactions into the much slower and more integrative biochemical reactions of the Calvin–Benson cycle and, eventually, into carbon budget of plants exposed to dynamic light environment.

## 2. Materials and methods

*Synechocystis* sp. PCC6803 was grown at 25 °C in BG11 medium [17] in batch cultures. The cell suspension (ca. 50 ml) in a 100-ml Erlenmeyer flask was stirred by an orbital shaker (ca. 150 min<sup>-1</sup>) under fluorescent tubes providing incident photon flux density (PFD) of ca. 25 μmol photons m<sup>-2</sup> s<sup>-1</sup>. The cells in late exponential growth phase were used for the experiments.

Tobacco (*Nicotiana tabaccum*, L.) was grown hydroponically in a growth chamber on 50% Knop solution at 25/20° and a 14/10 h day/night regime. The incident PFD at the top of the plants was 450 μmol photons m<sup>-2</sup> s<sup>-1</sup>. The fourth leaf attached to the plant was used in measurements.

### 2.1. Fluorescence emission of cyanobacteria

A double-modulation fluorometer [18] was custom-modified by Photon Systems Instruments, Ltd., Brno, Czech Republic ([www.psi.cz](http://www.psi.cz)) to provide harmonically modulated actinic light (620 or 465 nm) with period, mean PFD and modulation amplitude defined by instrument protocol. The 10-μs-long measuring flashes were generated by light-emitting diodes, orange (620 nm) by Agilent Technologies HLMP-EH08 and blue (465 nm) by Nichia NSPB500S. The flashes were repeated 100 times during each period of the actinic light modulation. The cell suspension was gently stirred in a standard 1 cm fluorescence cuvette with temperature stabilized by a Peltier-based thermoregulator (TR2000, Photon Systems Instruments). Fluorescence emission of the cells was carried by a fiber light guide to a SPEX 270 M Jobin Yvon monochromator (spectral dispersion 3.1 nm/mm with 1200 g/mm grating) where it was spectrally resolved (detection bandwidth 5 nm) before reaching a photomultiplier tube, Hamamatsu R2228 (Japan). The signal from the photomultiplier was captured in the 100 kHz, 16-bit port of the double-modulation fluorometer.

### 2.2. Gas exchange measurements with leaves

In a two-channel fast-response measurement system (Fast-Est, Tartu, Estonia; see Refs. [19,20]) a section of a leaf was enclosed in a sandwich-type chamber (diameter 31 mm, height 3 mm) where the gas flow rate was 0.5 mmol s<sup>-1</sup>. The upper side of the leaf was sealed by starch gel to the glass window of the chamber that was thermoregulated by circulating water at 22 °C. The gel thermal bridge increased the heat exchange coefficient between the leaf and the water bath to ca. 400 W m<sup>-2</sup> K<sup>-1</sup> so that the leaf

temperature did not exceed 22.5 °C during the light peaks, as calculated from the leaf energy budget.

Gas exchange occurred through the lower epidermis. The necessary O<sub>2</sub> and CO<sub>2</sub> concentrations were obtained by mixing pure gases at controlled flow rates and were 210 mmol mol<sup>-1</sup> (21%) and 360 μmol mol<sup>-1</sup> (360 ppm), respectively. The CO<sub>2</sub> concentration downstream of the chamber was measured by a LI-6251 CO<sub>2</sub> analyzer (LiCor, Lincoln, NE, USA). Humidity was controlled by passing an adjustable fraction of the gas over water at 50 °C and was measured by a psychrometer referenced to dry air. The vapor pressure deficit of the flushing gas was 1.7 kPa.

The leaf chamber was illuminated through a multiarm, randomized fiber light guide (Fast-Est). Schott KL 1500 tungsten halogen light source equipped with a heat-reflecting filter (Optical Coating Laboratory, Inc., Santa Rosa, CA) provided white actinic illumination. Another Schott KL1500 equipped with a heat-reflecting filter provided fluorescence saturation pulses of 11,000 μmol photons m<sup>-2</sup> s<sup>-1</sup>. A small fiber bundle in the light guide was connected to a LI-190 SB quantum sensor (LiCor) to provide a continuous recording of the incident actinic PFD.

Leaf absorption coefficient for the actinic light was measured with an integrating sphere and a spectroradiometer PC-2000 (Ocean Optics, Dunedin, FL). Rates of photon absorption were calculated by integrating the product of the absorption coefficient of the leaf times the PFD of the beam over the spectrum. The integrated absorption coefficient ranged from 0.8 to 0.85.

### 2.3. Chlorophyll fluorescence and leaf transmission at 820 nm

Two of the arms of the instrument light guide were used to measure Chl fluorescence by the ED-101 emitter–detector unit and 820 nm transmission by ED P700DW unit of two PAM 101 fluorometers (H. Walz, GmbH, Effeltrich, Germany). The sample port of the light guide was an ellipsoid of 1 × 2 cm<sup>2</sup> placed at a distance of 1 cm parallel to the leaf. The interference between the parallel measurement of Chl fluorescence and 820 nm transmission was prevented by an additional short-pass filter inserted in front of the fluorescence detecting ED-101 emitter–detector unit.

### 2.4. Operation of the system and data recording

The leaf system was operated and data were recorded using an A/D converter board ADIO 1600 (ICS Advent, San Diego, CA) and a system-operation and data-recording program RECO (Fast-Est). The harmonically modulated actinic light was generated by controlling the respective light source (KL 1500, Schott, Germany) with this program. Signals from the CO<sub>2</sub> analyzer, psychrometer, and the two PAM 101 were recorded at 5-ms intervals and data

points were plotted on the screen every 200 ms after averaging.

## 3. Results

### 3.1. Negative feedback regulation of the cyanobacterial antenna results in an upper harmonic modulation of the phycobilisome-mediated fluorescence emission

In dark-adapted cyanobacteria, the excitation energy is supplied to PSII reaction centers by an extrinsic light-harvesting complex, the phycobilisome, and by a small inner Chl *a* antenna. The excitation energy in the more abundant Photosystem I (PSI) is supplied by Chl *a* and carotenoids of the reaction center complex. Orange light that is strongly absorbed by phycobilisomes and weakly absorbed by chlorophylls and carotenoids leads to an unbalanced operation of the two photosystems which elicits a negative feedback de-coupling of the phycobilisomes from PSII (reviewed in Refs. [14,15]; also see a recent model [16]). The regulation of the energetic coupling of the phycobilisomes strongly affects the fluorescence emission yield [21–23]. Our earlier proposed hypothesis [13] suggests that, in harmonically modulated actinic irradiance, such a regulation can lead to upper harmonic modes in fluorescence emission yield.

Suspension of *Synechococcus* sp. PCC6803 was exposed to harmonically modulated orange actinic light ( $\lambda_{\max} = 620$  nm, frequency  $\omega = 2\pi/T = 2\pi/20$  s,  $I_{\min} \approx 40$  and  $I_{\max} \approx 360$  μmol photons m<sup>-2</sup> s<sup>-1</sup>) to elicit regulation of phycobilisome coupling to PSII. The broadband fluorescence emission yield ( $\lambda > 690$  nm) was first probed by blue ( $\lambda_{\max} = 465$  nm) measuring flashes exciting directly chlorophylls of the proximal antenna and the reaction centers, while bypassing the phycobilisomes (Fig. 1A). The variable fluorescence closely followed the incident irradiance. With increasing actinic light, more PSII reaction centers were closed by reduction of the primary quinone acceptor Q<sub>A</sub>, leading to a reduced photochemical quenching and to a higher fluorescence yield [24]. The deconvolution (Fig. 1B) of the fluorescence transient excited by blue flashes (Fig. 1A) confirms that there is only little upper harmonic modulation of the photochemical quenching. We conclude that the approximately linear response of the fluorescence emission yield observed with the blue light flashes was not perturbed by the expected regulation of the phycobilisome antenna, except for a small non-linear increase of the fluorescence emission yield which was observed around the minimum of the actinic light modulation (Fig. 1A).

In another experiment, we used again the orange actinic light to elicit the same changes in the Q<sub>A</sub> redox state and, consequently, in the PSII photochemical quenching as in Fig. 1A. Instead of probing the fluorescence yield by blue flashes as it was done in Fig. 1A, we used orange measuring

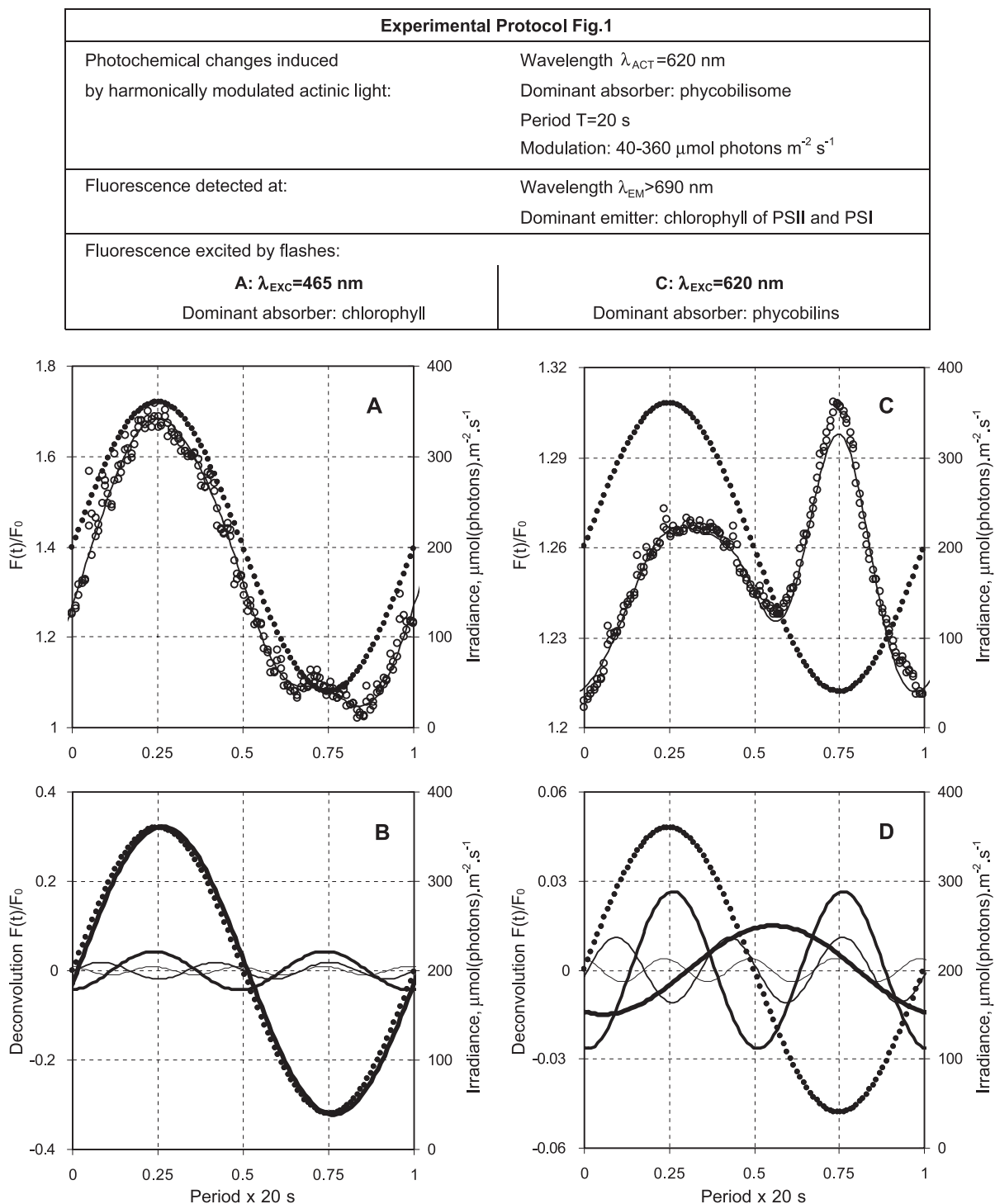


Fig. 1. Transients of the chlorophyll fluorescence yield (○) were measured in *Synechocystis* sp. PCC6803 exposed for 1 min to harmonically modulated irradiance oscillating between 40 and 360  $\mu\text{mol photons m}^{-2} \text{s}^{-1}$  for a period of 20 s. The wavelength of fluorescence measured was  $>690$  nm. The modulation of the incident actinic irradiance is shown by dotted line against the secondary Y-axis (right side ordinate). The dominant wavelength of the actinic light was 620 nm for both panels so that photochemical activities were always excited dominantly via phycobilisomes. The transients shown in Panels A and C differ only in the wavelength of the measuring flashes: (A) blue flashes of 465 nm excited directly chlorophyll; (C) orange flashes of 620 nm excited predominantly phycobilisomes. The transients are represented by the ratio of instantaneous fluorescence  $F(t)$  divided by  $F_0$  fluorescence measured in dark. The bottom panels (B,D) show the time course of irradiance (dotted line) and de-convolution of the measured fluorescence transients into fundamental harmonic component of the same frequency as the light modulation ( $\omega=2\pi/20$  s, heavy solid line) and of the three upper harmonic components ( $2\omega$ ,  $3\omega$ ,  $4\omega$ ), solid curves of decreasing thickness. Panel B shows the de-convolution of the transient measured with blue flashes and panel D with orange flashes.

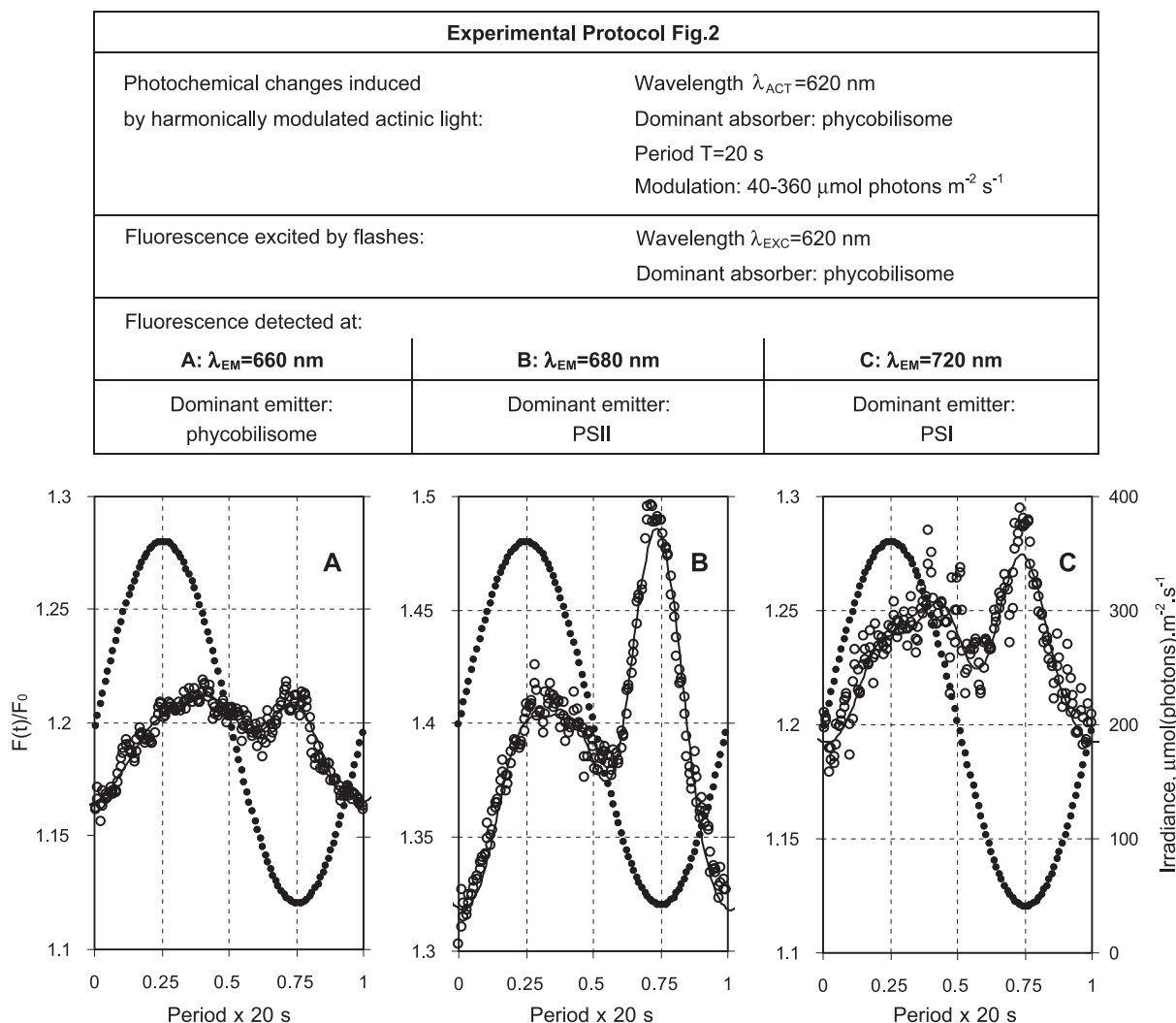


Fig. 2. Transients of the fluorescence yield (○) were measured at 660 nm (A), at 680 nm (B) and at 720 nm (C) in *Synechocystis* sp. PCC6803 exposed for 1 min to harmonically modulated irradiance oscillating between 40 and 360  $\mu\text{mol photons m}^{-2} \text{s}^{-1}$  for a period of 20 s. The dominant wavelength of the actinic light and of the measuring flashes was 620 nm in all three cases. Note different offset in Panel B compared to Panels A and C.

flashes ( $\lambda_{max}=620$  nm) that are primarily absorbed by phycobilisomes. Then, the fluorescence emission yield exhibited a non-linear modulation with strong upper harmonic modes (Fig. 1C).<sup>1</sup> The de-convolution of the fluorescence transient excited by the orange flashes (Fig. 1D) revealed that the sharp peak appearing in the fluorescence transient around the minimum of the incident irradiance (Fig. 1C) results from a constructive interference of the maxima of the upper harmonic modes. The temporal pattern of the fluorescence response is dominated by the  $2\omega$  upper harmonic component (Fig. 1D) that is largely responsible for the appearance of two distinct maxima in Fig. 1C. The

fundamental component of the fluorescence response ( $\omega$ , heavy line in Fig. 1D) is of smaller amplitude and significantly phase-shifted relative to the harmonically modulated irradiance (dotted line in Fig. 1).

The non-linear, upper harmonic modulation shown in Fig. 1C is caused by changes in the quantum yield of fluorescence emission that is mediated by phycobilisomes. These quantum yield changes are of a different nature than those observed with the blue light measuring excitation (Fig. 1A). We propose that the observed non-linearity reflects the regulatory un-coupling and re-coupling of the phycobilisome to PSII. The transient sharp increase in the phycobilisome-mediated Chl fluorescence emission yield in Fig. 1C can occur as a result of docking of phycobilisome to PSII that changes the emission yield without contributing significantly to PSII photochemistry.

In another experiment, we exposed the cyanobacteria to blue actinic irradiance instead of the orange actinic irradiance applied above. The blue actinic light excited directly

<sup>1</sup> Note the large difference between the ordinate scales in Fig. 1A and C. The ratio  $F_v/F_0$  in cyanobacteria is known to vary with the excitation wavelength due to the changing  $F_0$  contribution by the phycobilisomes and by the two photosystems. The large  $F_0$  fluorescence occurring with the orange measuring flashes is presumably caused by inclusion of phycobilisome emission that is independent of the photochemical activity in the reaction centers.

chlorophyll and did not lead to a PSII over-excitation via phycobilisomes. The upper harmonic modes in fluorescence were observed neither with blue nor with orange measuring flashes (not shown). This observation is consistent with our proposal that the upper harmonic modes appear in the fluorescence emission only as a result of the phycobilisome regulation in the orange actinic light.

### 3.2. The phycobilisome-mediated fluorescence exhibiting the strong upper harmonic modulation originates from photochemically inactive chlorophylls of PSII

The absence of a strong upper harmonic modulation in the photochemical quenching of the variable PSII fluorescence (Fig. 1A) and its clear presence in the phycobilisome-mediated fluorescence emission (Fig. 1C) suggest that the latter non-linearity can be caused by phycobilisome regulation that is either affecting directly the fluorescence yield of the extrinsic antenna or that is affecting fluorescence emission from PSI or, finally, that is modulating fluorescence yield of PSII chlorophyll that is not engaged effectively in the energy transfer to the reaction centers. To probe which of these is the most likely alternative, we measured fluorescence emission resolving three wavelength-bands so that transients originating in the two photosystems and in the phycobilisome antenna could be distinguished (Fig. 2). The upper harmonic modulation was the weakest in the emission predominantly originating from phycobilisomes (660 nm, Fig. 2A) and the strongest in the range of dominant PSII emission (680 nm, Fig. 2B). The temporal pattern of the fluorescence yield measured at 720 nm (Fig. 2C), although appearing with lower amplitude, was similar to that at 680 nm (Fig. 2B).<sup>2</sup>

This conclusion was further supported by a more detailed measurement of the upper harmonic modulation where the sum of the amplitudes of the upper harmonic components (frequencies  $2\omega$ ,  $3\omega$ ,  $4\omega$ ) was normalized to the amplitude of the fundamental component (frequency  $\omega$ ) and plotted as a function of the emission wavelength with a high resolution (Fig. 3). The maximum of the relative amplitudes of the upper harmonic modes was found at ca. 680–685 nm, which is the emission dominantly ascribed to chlorophylls of PSII (reviewed in Ref. [25]). This further supports our conclusion that the fluorescence with the phycobilisome-mediated upper harmonic modulation originates in PSII.

### 3.3. Tobacco leaves respond to harmonic forcing by a strong upper harmonic modulation of photosynthetic activities

Numerous negative feedback mechanisms are expected to maintain the homeostasis of the photosynthetic reactions

<sup>2</sup> No depression in 720 nm emission, which would correspond to the enhancement of 680 nm emission, or a vice versa effect was observed. We suggest that the regulation of phycobilisome energetic coupling in the harmonically modulated light does not include antiparallel changes in the PSI excitation that would be expected in the case of mobile phycobilisomes that functionally attach to PSI soon after detaching from PSII.

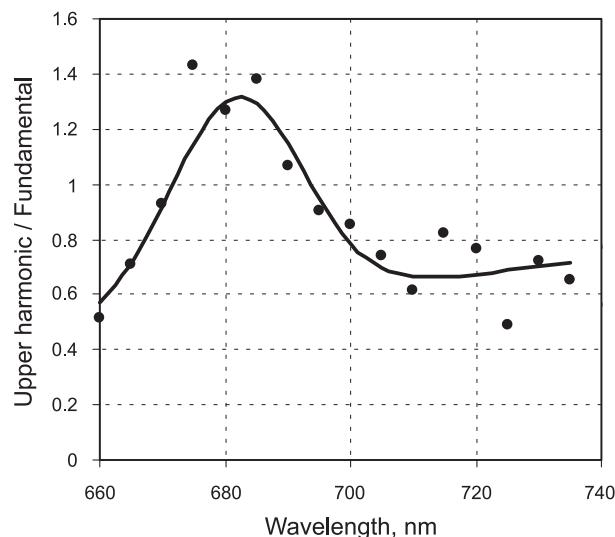


Fig. 3. Sum of the amplitudes of the upper harmonic components (frequencies  $2\omega$ ,  $3\omega$ ,  $4\omega$ ) was normalized to the amplitude of the fundamental component (frequency  $\omega$ ) and plotted as a function of the emission wavelength. The bandwidth of the detection was 5 nm. The harmonic forcing was achieved and fluorescence was excited using the same experimental protocol as in Fig. 2.

also in higher plants. Based on the earlier prediction from reversed engineering analysis [13] and based on the experiments with cyanobacteria reported above, we propose that the regulation will cause an upper harmonic modulation of photosynthetic activities in higher plants. Here, we investigate if this modulation occurs only at the level affecting the primary photochemistry or if it reaches up to the slower and more integrative reactions of the Calvin–Benson cycle.

First, we exposed tobacco leaves to white PFD oscillating harmonically between ca. 20 and 800  $\mu\text{mol photons m}^{-2} \text{s}^{-1}$  with a period of 60 s. The period was selected to be close to the period of autonomous oscillations [9] and close to the resonance period of the forced oscillations [13]. In agreement with our earlier results [13], a complex periodic transient was found in fluorescence emission (Fig. 4A). The fluorescence transient was fitted by a steady-state component plus four harmonic components (Fig. 4B): one fundamental ( $\omega = 2\pi/60 \text{ s}^{-1}$ ) and by three upper harmonic components ( $2\omega$ ,  $3\omega$ ,  $4\omega$ ). A complex transient consisting of a fundamental and several upper harmonic components was also found (not shown) in the absorption measured at 820 nm that dominantly reflects the redox state of the primary donor of PSI [26].

Most relevant, the upper harmonic modulation was detected not only in fluorescence and in  $\Delta 820$  signals but also in the rate of  $\text{CO}_2$  assimilation. A sharp peak in the rate of  $\text{CO}_2$  assimilation appears (Fig. 4D) at about the same phase as the maximum of Chl fluorescence emission (Fig. 4A) followed by an oscillatory decline to a minimum reached with a significant delay after the minimum of the fluorescence emission yield. The fitting of the measured  $\text{CO}_2$  assimilation (Fig. 4E) reveals that, similarly to Chl fluorescence (Fig. 4B), the rate of  $\text{CO}_2$  assimilation can be de-convoluted into a

steady-state component, fundamental harmonic component of the same frequency with the irradiance and into, at least, three upper harmonic components. The fundamental harmonic component is only slightly delayed relative to the irradiance (Fig. 4E) and represents the assimilation that is proportional to the irradiance with a delay caused by filling of the metabolite pools. Subtracting the fundamental harmonic component from the measured transient of the assimilation rate reveals explicitly the upper harmonic oscillatory modulation of large amplitude (Fig. 4F, closed circles).

The molecular processes responsible for the non-linear, upper harmonic modulation of the fluorescence emission and of the CO<sub>2</sub> assimilation can involve NPQ as well as changes in the photochemical quantum yield induced by fluctuating electron flow. To discriminate between the two alternatives, we measured during the entire period of harmonic forcing not only the instantaneous yield of Chl fluorescence emission  $F(t)$  but also its maximal yield  $F'_M(t)$  when all PSII reaction centers were transiently closed by flash of light reducing the plastoquinone pool.<sup>3</sup> The instantaneous quantum yield of PSII was estimated using  $\Phi_{II}(t) \approx (F'_M(t) - F(t))/F'_M(t)$  [27] and the NPQ was quantified by  $\text{NPQ}(t) = (F_M - F'_M(t))/F'_M(t)$  [28].

Both, the photochemical quenching and NPQ contributed significantly to the fluorescence transient (Fig. 4C). In the low light phase at the beginning of the period, the CO<sub>2</sub> uptake (Fig. 4D) and the electron transport rate increased with light, accompanied by a gradually increasing fluorescence (Fig. 4A). The PSII yield,  $\Phi_{II}$ , only slowly decreased from its maximum (full circles, Fig. 4C), while the NPQ remained low (open circles, Fig. 4C). At PFD reaching ca. 600  $\mu\text{mol photons m}^{-2} \text{s}^{-1}$ , the fluorescence increase was greatly accelerated as if significantly more electrons were released from water by PSII than accepted by PSI. The Chl fluorescence yield reached a sharp maximum at 0.4 of the period (ca. 24th second) when the irradiance was at ca. 690  $\mu\text{mol photons m}^{-2} \text{s}^{-1}$  (Fig. 4A). At the same time, the rate of CO<sub>2</sub> uptake also reached a maximum (Fig. 4D). The congestion of the electron transport chain between the two photosystems (i.e., the reduction of the intersystem electron transport carriers), which was indicated by the high Chl fluorescence, prompted a rapid onset of NPQ (open circles, Fig. 4C). Under the oscillating irradiance,  $F'_m$  never approached the maximum dark-adapted  $F_m$ , and stayed much lower, even during the minimum of irradiance when the lowest NPQ of 2.4 was observed. We propose that the slow components of the NPQ stayed high throughout the oscillation period and only the energy-dependent  $q_E$ -type NPQ [29] responded fast enough to follow the irradiation change. The time constant of this fast component was about 15 s (0.25 of the period) reflecting the time interval during

which regulatory elevated  $\Delta\text{pH}$  was generated across the thylakoid membrane in response to the congestion of electron transport at the PSI acceptor side. The increased NPQ reduced the excitation of PSII leading to the subsequent decline in fluorescence and as well as to decline in the CO<sub>2</sub> uptake rate (Fig. 4A,D). The kinetics of the decline of the CO<sub>2</sub> assimilation rate and of the Chl fluorescence emission were strongly modulated by upper harmonic modes that reflected downstream oscillations, possibly in the redox-controlled reactions of the Calvin–Benson cycle [30].

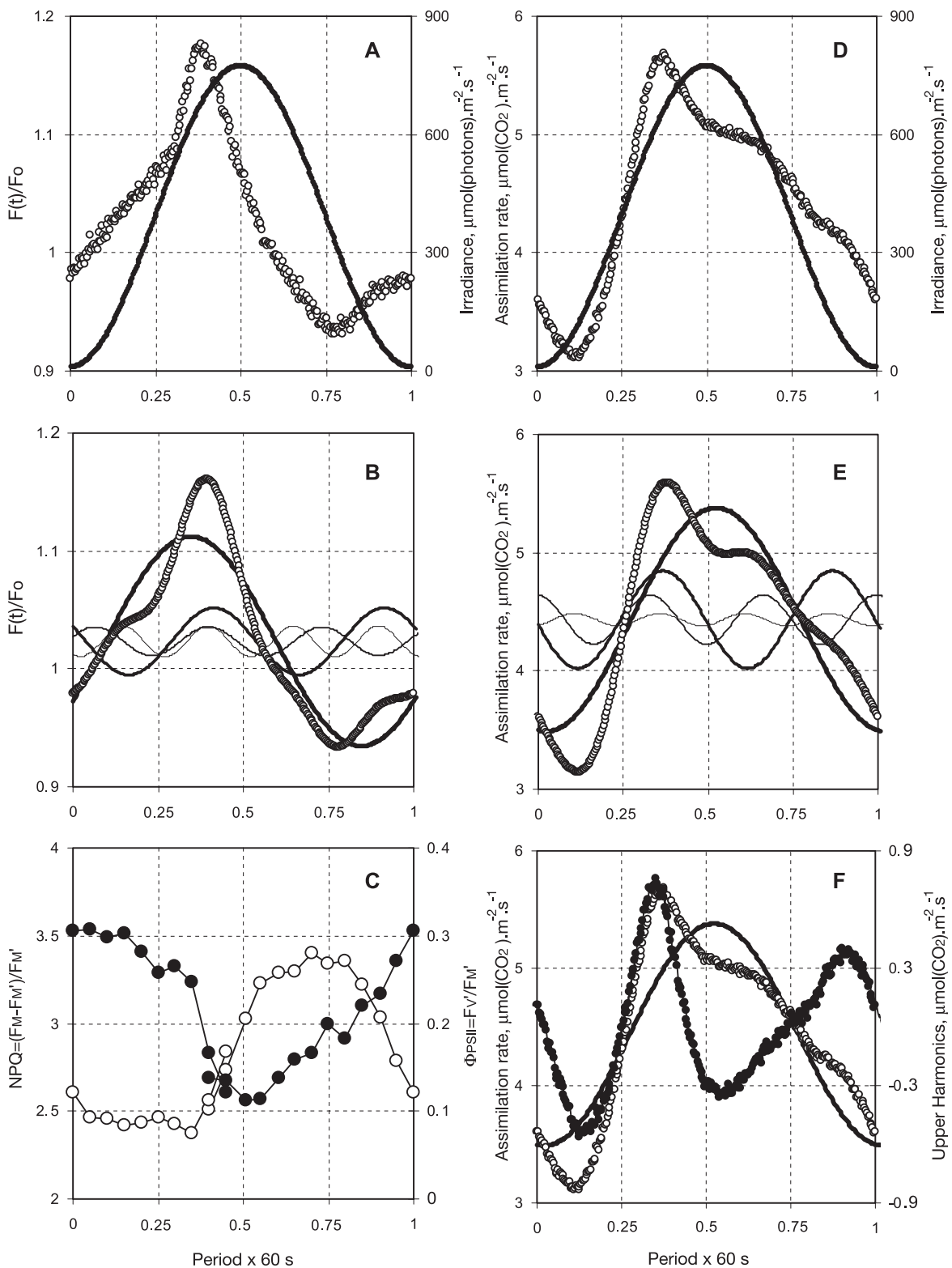
Throughout the entire period of the harmonic forcing, the modulation of the photochemical yield,  $\Phi_{II}$ , preceded that of the NPQ. Based on this observation, we propose that the observed complex non-linear modulation of the photosynthetic activities is primarily due to oscillatory variations in the electron flow rate induced by the harmonically modulated irradiance. The regulatory feedback loops induce the upper harmonic modes in electron flow similarly to the regulation of the phycobilisome energetic coupling in cyanobacteria that is documented above.

### 3.4. The complex modulation of photosynthesis is determined by the temporal pattern rather than by the amplitude of the harmonically modulated light

The character of the transients found in the Chl fluorescence emission (Fig. 4A) and in the CO<sub>2</sub> assimilation rate (Fig. 4D) indicates that oscillations rather than an incoherent forward filling of the metabolite pools are the memory effects affecting dominantly the dynamics of plant photosynthesis in harmonically modulated irradiance. To further test this hypothesis, we compared the plant response to harmonically modulated irradiance of largely different amplitudes.

In the transients shown in Fig. 4, the sharp maxima of the Chl fluorescence emission yield and of the CO<sub>2</sub> assimilation as well as the onset of NPQ of Chl fluorescence appear during the phase of the harmonic forcing when the irradiance rises above 600  $\mu\text{mol photons m}^{-2} \text{s}^{-1}$ . If determined by this critical irradiance, the complex non-linear transients should be absent with an oscillating light that has a maximum below 600  $\mu\text{mol photons m}^{-2} \text{s}^{-1}$ . Instead, Fig. 5 shows complex non-linear kinetics of Chl fluorescence emission, rate of CO<sub>2</sub> assimilation and of P700 redox changes (approximated by the absorption changes at 820 nm [31]) in leaves exposed to harmonically modulated light of photon flux densities that are significantly lower than 600  $\mu\text{mol photons m}^{-2} \text{s}^{-1}$ . In the light oscillating between 20 and 400  $\mu\text{mol photons m}^{-2} \text{s}^{-1}$ , the sharp increase in Chl fluorescence begins at the light level of 200  $\mu\text{mol photons m}^{-2} \text{s}^{-1}$  and the peak in CO<sub>2</sub> uptake occurs at 350  $\mu\text{mol photons m}^{-2} \text{s}^{-1}$  (Fig. 5A,B). With the amplitude of the harmonically modulated light further decreased to 200  $\mu\text{mol photons m}^{-2} \text{s}^{-1}$ , the maxima of the Chl fluorescence emission (Fig. 5D) and of the CO<sub>2</sub> assimilation (Fig. 5E) are delayed relative to the corresponding maxima in stronger light and coincide with the maximum of irradiance.

<sup>3</sup> In order to minimize interference by saturation pulses, the period of pulsing was chosen 1.05 times the period of the actinic illumination. Thus, only one saturating pulse was given in each period. Over 20 periods, the pulses covered the whole sine wave.



The  $\Delta 820$  signal is also strongly modulated during the period of the actinic light with P700<sup>4</sup> fully reduced close to

<sup>4</sup> Here, we assume that the  $\Delta 820$  signal is dominantly caused by redox changes of the primary donor of PSI (P700). However, plastocyanin can also contribute partly to the measured signals [29].

the minimum of the actinic irradiance and partially oxidized in high light phase (Fig. 5C,F). This initially nearly linear relationship between the actinic irradiance and the signal reflecting the oxidation of PSI donor side (mainly plastocyanin oxidation is expected to occur at these limiting irradiances) is perturbed by a distinct non-linear feature

occurring always in parallel to the sharp maximum of Chl fluorescence emission (cf. Fig. 5A with C and Fig. 5D with F). We propose that the non-linearity is caused by the transient congestion of the electron transport chain (i.e., reduction of all intermediates up to the electron acceptor of PSI, referred to in the literature as traffic jam of electrons [32]) leading simultaneously to the increased Chl fluorescence emission and to the increased reduction of P700 and of plastocyanin that is another contributor to the  $\Delta 820$  signal [31,33]. The congestion of the electron flow occurs when the Calvin–Benson cycle operates at its maximum rate but cannot process the fluxes that are steadily increasing with the increasing irradiance (Fig. 4D). The imbalance between the incoming fluxes and the processing capacity of the Calvin–Benson cycle leads to a signal rapidly increasing the NPQ of Chl fluorescence (Fig. 4C) and causing P700 oxidation, as seen from the steep trough in the 820 nm signal (Fig. 5C). In the actinic light oscillating between 20 and 800  $\mu\text{mol photons m}^{-2} \text{s}^{-1}$ , the maximum in fluorescence occurred at 0.4 of the 60 s period (ca. 24th second) when the actinic light is increased to about 690  $\mu\text{mol photons m}^{-2} \text{s}^{-1}$  (Fig. 4A). With the lower light oscillating between 20 and 400  $\mu\text{mol photons m}^{-2} \text{s}^{-1}$ , the maximum of the fluorescence yield occurred at 0.38 of the period (23rd second) when the irradiance reached ca. 340  $\mu\text{mol photons m}^{-2} \text{s}^{-1}$  (Fig. 5A). In the light oscillating between 20 and 200  $\mu\text{mol photons m}^{-2} \text{s}^{-1}$ , the fluorescence maximum coincided approximately with the maximum of the actinic irradiance at 0.5 of the period (30th second).

The small quantitative differences do not obscure similarities in the dynamics of the photosynthetic processes in all three light regimes. The transients exhibit qualitatively similar features with decreasing resolution of the upper harmonic modulation towards the low irradiance: the most pronounced upper harmonic modulation was found with the oscillating light 20–800  $\mu\text{mol photons m}^{-2} \text{s}^{-1}$  (Fig. 4) and the least explicit in 20–200  $\mu\text{mol photons m}^{-2} \text{s}^{-1}$  (Fig. 5).

The qualitatively similar features in the transients in Figs. 4 and 5 are consistent with the notion that the harmonically modulated light forces fundamental and upper harmonic oscillations in biochemical reactions. The effect of such a forcing is expected to depend strongly on the frequency of the forcing and only to a lesser extent on the amplitude of the light modulation.

### 3.5. The photosynthetic transients are largely determined by the frequency of the harmonically modulated light

Indeed, the patterns of transients observed in harmonically modulated light of high frequency ( $\omega = 2\pi/20 \text{ s}^{-1}$ , Fig. 6A,B) and of low frequency ( $\omega = 2\pi/300 \text{ s}^{-1}$ , Fig. 6C,D) are significantly different from the patterns observed in the medium frequency light (Figs. 3 and 4). In the rapidly modulated actinic light, the fluorescence yield exhibits strong upper harmonic modes (Fig. 6A). These rapid fluctuations are integrated by the slower biochemical reactions of the Calvin–Benson cycle and, consequently, the rate of  $\text{CO}_2$  assimilation changes linearly with changing light (Fig. 6B). In the slowly modulated light (Fig. 6D), the rate of  $\text{CO}_2$  assimilation increases slowly with the increasing light to saturation that is already corrected by a substantial NPQ. The assimilation rate remains high until the light drops below the saturation level and after the metabolites generated during the high irradiance phase are exhausted. The fluorescence transient (Fig. 6C) remains very complex even with the low frequency of forcing.

## 4. Discussion

The experiments with the cyanobacterium *Synechocystis* sp. PCC 6803 verified the causal relationship between a negative feedback regulation and appearance of the upper harmonic, non-linear modulation of Chl fluorescence emission. The negative feedback regulation of the photosynthetic antenna was induced by orange, harmonically modulated light that excited dominantly the phycobilisome antenna. When the actinic light was high, the PSII was over-excited compared to PSI sending a signal to functionally detach the phycobilisome from PSII. Before the functional detachment was completed, the modulated actinic light was already steeply declining. The discrepancy between the detaching phycobilisome and the steeply declining actinic light is suggested to lead to a re-coupling of the extrinsic antenna back to PSII that is visualized by the sharp maximum of the PSII fluorescence emission yield excited via phycobilisomes in Fig. 1C. We suggest that it is a conformational change during docking of the phycobilisome to PSII that transiently increases the PSII

Fig. 4. Transients of the chlorophyll fluorescence yield (A) and of the rate of  $\text{CO}_2$  assimilation (D) were elicited in a tobacco leaf by white light that was harmonically oscillating between 20 and 800  $\mu\text{mol photons m}^{-2} \text{s}^{-1}$  with a frequency  $\omega = 2\pi/60 \text{ s}^{-1}$ . The transients are shown relative to the phase of the irradiance modulation that started at the irradiance minimum (0 of the period), continued to the maximum (0.5 of the period) and ended at the next minimum (1 of the period). Panel A shows the measured chlorophyll fluorescence yield (A, open circles) during one period of the harmonically modulated light (A, solid line). The numerical fit of the fluorescence emission data of Panel A, shown in Panel B (open circles), was calculated by a least-square-deviation procedure using a constant offset superimposed by four harmonic components. The fundamental component ( $\omega = 2\pi/60 \text{ s}^{-1}$ ) is shown by the thick line and the three upper harmonic components ( $2\omega$ ,  $3\omega$  and  $4\omega$ ) are represented by solid lines of decreasing thickness in Panel B. Panel C shows the photochemical yield estimated from the fluorescence emission  $\Phi_{II}(t) \approx (F_M(t) - (t))/F_M(t)$  (closed circles) and the NPQ  $= (F_M - F_M(t))/F_M(t)$  (closed circles) during one period of the light modulation. The measured rate of  $\text{CO}_2$  assimilation (open circles) together with the irradiance (solid line) are shown in Panel D. The corresponding numerical fit of data of Panel D is shown in Panel E by open circles. Panel E also shows de-convolution of the fit into the fundamental and three upper harmonic components (solid lines of decreasing thickness). The measured rate of  $\text{CO}_2$  assimilation (open circles) and the fundamental component of the numerical fit (solid line) are repeated in Panel F and shown together with the net upper harmonic modulation (closed circles) calculated by subtracting the fundamental component (solid line) from the measured transient (open circles).

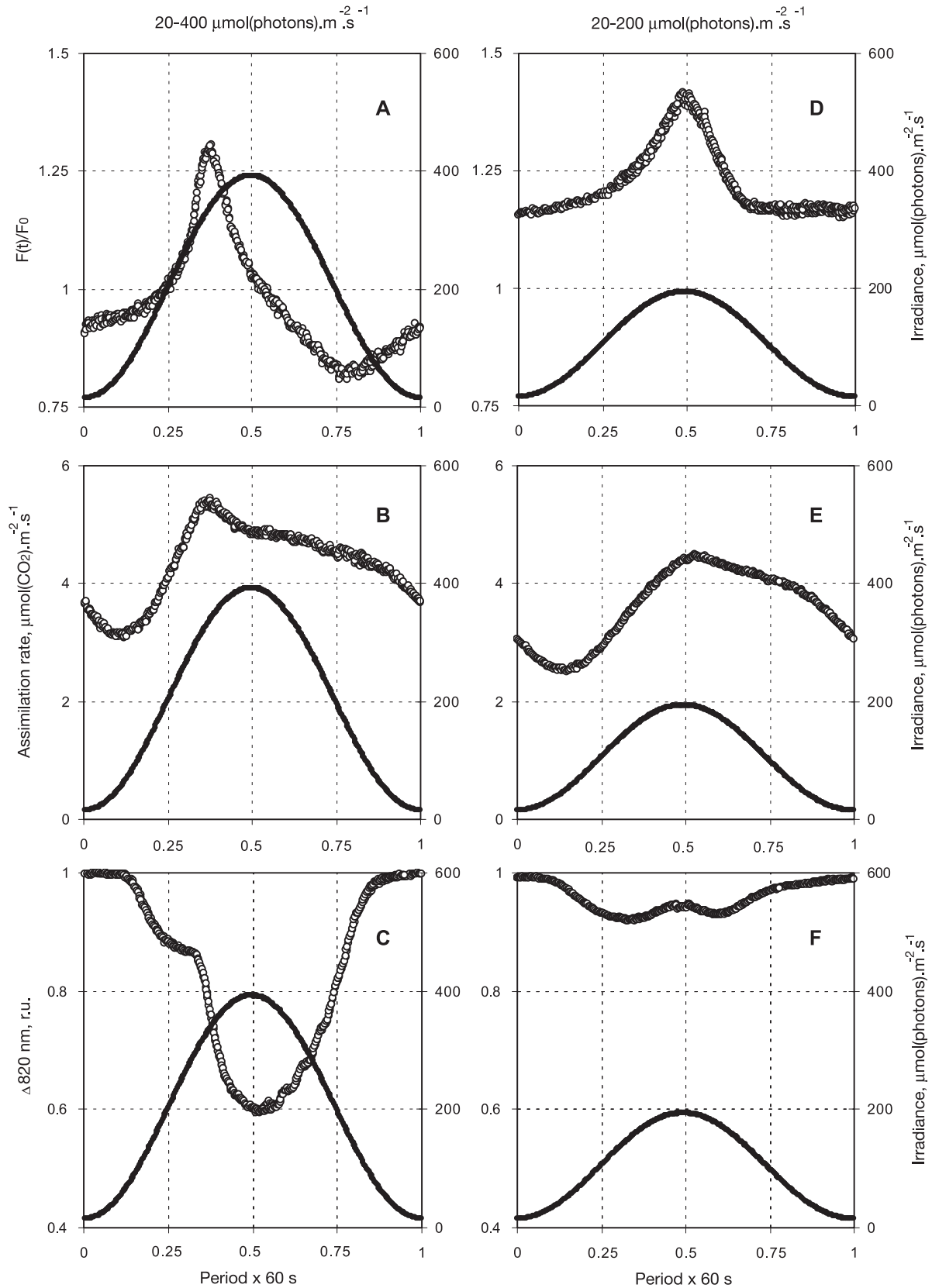


Fig. 5. Transients (open circles) of the chlorophyll fluorescence  $F(t)/F_0$  (A,D), of the rate of  $\text{CO}_2$  assimilation (B,E) and of the  $\Delta 820 \text{ nm}$  absorption signal (C,F) in tobacco leaf during a period of harmonically modulated irradiance (solid line in all panels) of 60 s period. The panels A, B and C show transients in light oscillating between 20 and 400  $\mu\text{mol photons m}^{-2} \text{s}^{-1}$  and the panels D, E and F represent oscillations between 20 and 200  $\mu\text{mol photons m}^{-2} \text{s}^{-1}$ .

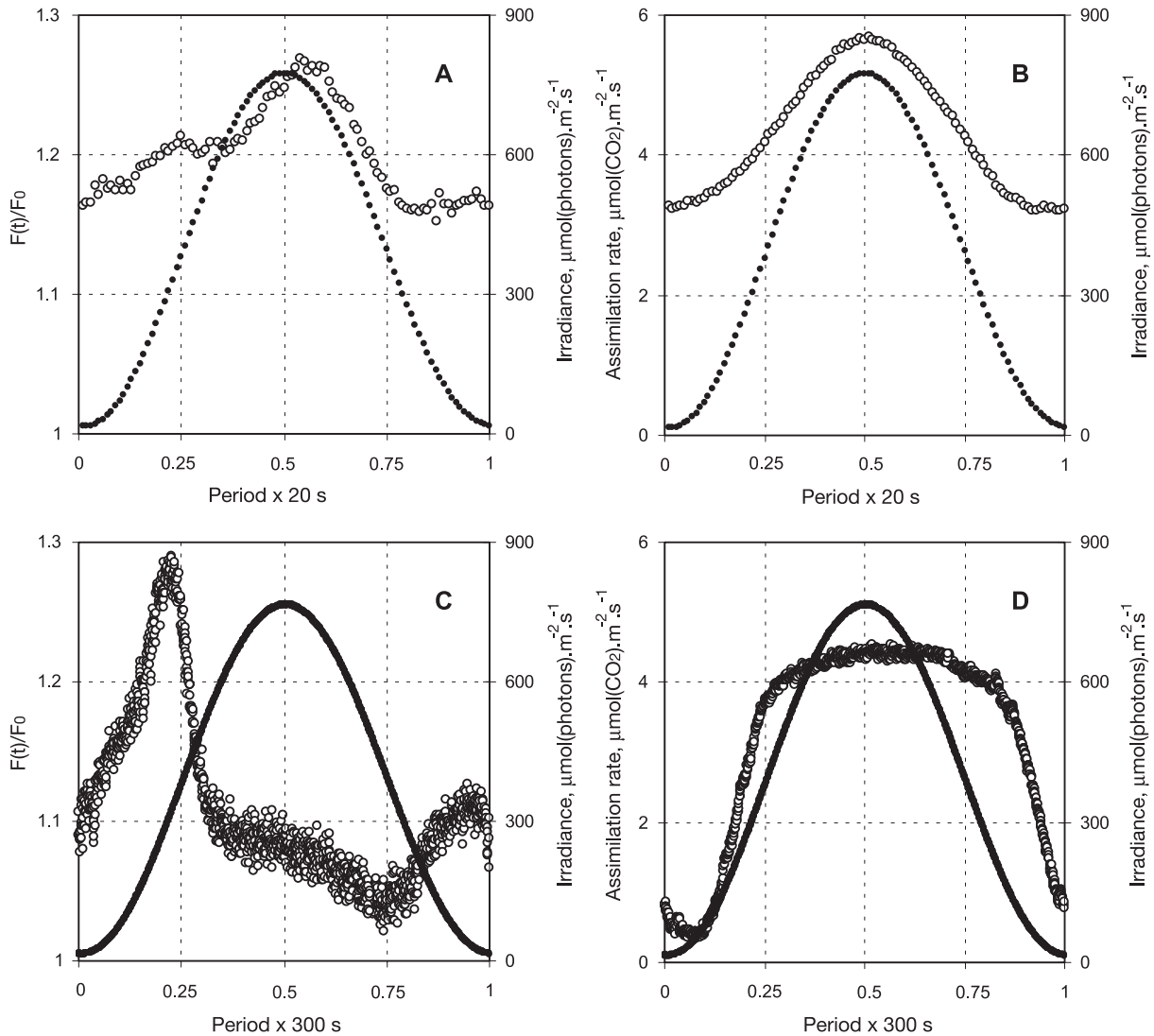


Fig. 6. The transients of chlorophyll fluorescence emission (A,C) and of the rate of  $\text{CO}_2$  assimilation (B,D) in light oscillating between 20 and  $800 \mu\text{mol photons m}^{-2} \text{s}^{-1}$  for a period of 20 s (A,B) and 300 s (C,D). The profile of the light modulation is shown in all panels by closed circles (merged into solid line in D).

fluorescence yield (sharp peak in Fig. 1C) without increasing the fraction of reduced  $Q_A$  by an increased energy transfer and by increased photochemical activity (absence of the sharp peak in Fig. 1A).

The experiments also led to an interesting result by showing that the highly dynamic changes in the emission of PSII that were caused by regulation of phycobilisome functional coupling were not accompanied by antiparallel changes in the PSI fluorescence emission (Fig. 2). Such an antiparallel modulation would be expected if the phycobilisomes detached from PSII had moved to PSI. Our experiments do not support such a model. On the time scale investigated here, the phycobilisomes detached from PSII may not serve PSI. The excitation energy captured by the detached phycobilisomes is non-radiatively dissipated. However, we cannot exclude that the energetic coupling of phycobilisomes to PSI occurs on a time scale significantly

exceeding the period of harmonic modulation applied here [15].

In the experiments with tobacco, we recorded  $\text{CO}_2$  uptake, Chl fluorescence and 820 nm transmission on the background of harmonically modulated white actinic light. The plant response measured by  $\text{CO}_2$  uptake exhibited a distinctly resonant character. The upper harmonic modes were absent in the rapidly modulated light ( $\omega = 2\pi/20 \text{ s}^{-1}$ , Fig. 6B), were strong with the medium-frequency modulation ( $\omega = 2\pi/60 \text{ s}^{-1}$ , Fig. 4D) and were reduced in the slowly modulated light ( $\omega = 2\pi/60 \text{ s}^{-1}$ , Fig. 6D).

The linear relationship between the  $\text{CO}_2$  uptake and the incident irradiance was observed in the rapidly modulated light ( $\omega = 2\pi/20 \text{ s}^{-1}$ , Fig. 6B) in spite of the strong upper harmonic modulation detected in the Chl fluorescence transients measured at the same frequency of modulation (Fig. 4A). We propose that the non-linear

modulation detected in fluorescence was smoothed away in the CO<sub>2</sub> uptake by an integration of the fast oscillatory components by slow reactions of the Calvin–Benson cycle.

In contrast, a strong non-linear, upper harmonic modulation of the CO<sub>2</sub> uptake was observed in the response elicited by the medium frequency of the light modulation ( $\omega = 2\pi/60 \text{ s}^{-1}$ , Fig. 4D). The Chl fluorescence transient and the P700 redox kinetics documented a transient congestion of the electron transport chain (i.e., reduction of all the electron carriers) appearing several seconds before the maximum irradiance was reached. At this phase, the Chl fluorescence yield and CO<sub>2</sub> uptake reached a sharp maximum before regulatory mechanisms relieving the electron transport congestion became effective. The regulation included the onset of NPQ (Fig. 4C) and oxidation of P700 (Fig. 5C), both indicating that regulatory  $\Delta\text{pH}$  was rapidly increased in response to the congestion of electron transport [34]. This supports the notion that proton-transporting cyclic electron transport around PSI is activated in response to increased electron pressure at the PSI acceptor side [35]. As a result of this, PSI takes the lead in regulation of PSII electron transport via the mechanism of NPQ [36] and in the regulation of the electron transport between the two photosystems via the photosynthetic control of plastoquinol oxidation [34].

In the slowly modulated light, the Chl fluorescence maximum resulting from the transient congestion of the electron transport chain appeared in the phase of the light increase (ca. 60 s after the minimum of the irradiance and 90 s before the maximum) when the CO<sub>2</sub> uptake already reached its steady-state level ( $\omega = 2\pi/300 \text{ s}^{-1}$ , Fig. 6C,D). The ensuing regulation had no effect on the steady-state rate of the CO<sub>2</sub> uptake and, consequently, no oscillations were observed in the assimilation.

We propose that the upper harmonic components reflect real metabolic oscillations rather than only correct for a non-linearity in the plant response to the changing irradiance (see also discussion in Ref. [13]). The upper harmonic modulation occurs in CO<sub>2</sub> uptake when the frequency of forcing resonates with the internal frequency of regulation in Calvin–Benson cycle. The non-linear, upper harmonic modulation occurs in a wide range of irradiance amplitudes (Figs. 4 and 5) further supporting the notion of dynamically driven oscillations over a model of an amplitude-controlled down-regulation.

Interestingly, our present model of photosynthesis [37–39] does not yield upper harmonic modulation of the photosynthetic activities in harmonically modulated irradiance (not shown). Similarly, the model fails to predict the autonomous photosynthetic oscillations found earlier (reviewed in Ref. [9]). These failures of the present models indicate a major gap in our understanding of photosynthetic dynamics. We expect that this information gap can be filled by further research on forced photosynthetic oscillations that are more easily induced than autonomous oscillations

and that also yield more information including a detailed frequency analysis of amplitudes and phases. We believe that the forced oscillations will become a major system-analysis tool in biology similar to their role in electrical engineering and in other fields dealing with complex systems [40]. Plants represent an exquisite model system that can be approached by this tool because their energetic machinery is driven by light which is easy to modulate within a wide range of frequencies and amplitudes and chlorophyll fluorescence is an intrinsic probe signal that communicates the dynamism of the system exposed to the harmonic forcing.

## Acknowledgements

LN, VB, FA and DS were supported in part by the grants LN00A141 and MSM123100001 of the Czech Ministry of Education and by the AV0Z6087904 project of Institute of Landscape Ecology CAS. AL and VO were supported by grant 5236 from the Estonian Science Foundation, AL was supported by Research Professor grant from the Estonian Academy of Science. The visit of LN to Tartu was supported by the Centre of Excellence on Molecular and Environmental Biology at Tartu University. The visit of Govindjee to Nove Hradky was supported by the grant LN00A141 of the Czech Ministry of Education. The technical assistance of Peter Vaczi is appreciated.

## References

- [1] R. Chazdon, Sunflecks and their importance to forest understory plants, *Adv. Ecol. Res.* 18 (1988) 1–63.
- [2] R.W. Pearcy, R.L. Chazdon, L.J. Gross, K.A. Mott, Photosynthetic utilization of sunflecks—a temporally patchy resource on a time scale of seconds to minutes, in: M. Caldwell, R. Pearcy (Eds.), *Exploitation of Environmental Heterogeneity by Plants*, Academic Press, San Diego, 1994, pp. 175–208.
- [3] B. Kroon, Variability of Photosystem II quantum yield and related processes in *Chlorella pyrenoidosa* (Chlorophyta) acclimated to an oscillating light regime simulating a mixed photic zone, *J. Phycol.* 30 (1994) 841–852.
- [4] H. Schubert, H. Matthijs, L. Mur, U. Schiewer, Blooming of cyanobacteria in turbulent water with steep light gradients: the effect of intermittent light and dark periods on the oxygen evolution of *Synechocystis* sp. PCC 6803, *FEMS Microbiol. Ecol.* 18 (1995) 237–245.
- [5] U. Hansen, J. Kolbowski, H. Dau, Relationship between photosynthesis and plasmalemma transport, *J. Exp. Bot.* 38 (1987) 1965–1981.
- [6] L. Ljung, *System Identification: Theory for the User*, PTR Prentice Hall, Engelwood Cliffs, NJ, 1991.
- [7] A. Laisk, K. Siebke, U. Gerst, H. Eichelmann, V. Oja, U. Heber, Oscillations in photosynthesis are initiated and supported by imbalances in the supply of ATP and NADPH to the Calvin cycle, *Planta* 185 (1991) 554–562.
- [8] A. Laisk, V. Oja, D. Walker, U. Heber, Oscillations in photosynthesis and reduction of Photosystem I acceptor side in sunflower leaves—functional cytochrome *b<sub>6</sub>/f*-Photosystem I ferredoxin-NADP reductase supercomplexes, *Photosynthetica* 27 (1992) 465–479.

- [9] D. Walker, Concerning oscillations, *Photosynth. Res.* 34 (1992) 387–395.
- [10] K. Siebke, E. Weis, Imaging of chlorophyll-*a* fluorescence in leaves—topography of photosynthetic oscillations in leaves of *Glechoma hederacea*, *Photosynth. Res.* 45 (1995) 225–237.
- [11] L. Fridlyand, Independent changes of ATP/ADP or  $\Delta\text{pH}$  could cause oscillations in photosynthesis, *J. Theor. Biol.* 193 (1998) 739–741.
- [12] N. Ferimazova, H. Küpper, L. Nedbal, M. Trtílek, Insights into photosynthetic oscillations on a single-cell level by two-dimensional microscopic measurements of chlorophyll fluorescence kinetics, *Photochem. Photobiol.* 76 (2002) 501–508.
- [13] L. Nedbal, V. Brezina, Complex metabolic oscillations in plants forced by harmonic irradiance, *Biophys. J.* 83 (2002) 2180–2189.
- [14] Y. Fujita, A. Murakami, K. Aizawa, K. Ohki, Short-term and long-term adaptation of the photosynthetic apparatus: homeostatic properties of thylakoids, in: D. Bryant (Ed.), *The Molecular Biology of Cyanobacteria*, Kluwer Academic Publishers, Dordrecht, 1994, pp. 677–692.
- [15] C. Mullineaux, How do cyanobacteria sense and respond to light? *Mol. Microbiol.* 41 (2001) 965–971.
- [16] M. McConnell, R. Koop, S. Vasil'ev, D. Bruce, Regulation of the distribution of chlorophyll and phycobilin-absorbed excitation energy in cyanobacteria. A structure-based model for the light state transition, *Plant Physiol.* 130 (2002) 1201–1212.
- [17] R. Stanier, R. Kunisawa, M. Mandel, G. Cohen-Bazire, Purification and properties of unicellular blue-green algae, *Bacteriol. Rev.* 35 (1971) 171–205.
- [18] M. Trtílek, D. Kramer, M. Koblížek, L. Nedbal, Dual-modulation LED kinetic fluorometer, *J. Lumin.* 72–74 (1997) 597–599.
- [19] A. Laisk, V. Oja, Dynamic gas exchange of leaf photosynthesis, *Measurement and Interpretation*, CSIRO Publishing, Canberra, 1998.
- [20] A. Laisk, V. Oja, B. Rasulov, H. Rämme, H. Eichelmann, I. Kasparova, H. Pettai, E. Padu, E. Vapaavuori, A computer-operated routine of gas exchange and optical measurements to diagnose photosynthetic apparatus in leaves, *Plant Cell Environ.* 25 (2002) 923–943.
- [21] C. Vernotte, C. Astier, J. Olive, State-1–State-2 adaptation in the cyanobacteria *Synechocystis* PCC-6714 wild type and *Synechocystis* PCC-6803 wild type and phycocyanin-less mutant, *Photosynth. Res.* 26 (1990) 203–212.
- [22] D. Campbell, V. Hurry, A. Clarke, P. Gustafsson, G. Oquist, Chlorophyll fluorescence analysis of cyanobacterial photosynthesis and acclimation, *Microbiol. Mol. Biol. Rev.* 62 (1998) 667–683.
- [23] M. Koblížek, J. Komenda, J. Masojídek, State transitions in the cyanobacterium *Synechococcus* PCC7942. Mobile antenna or spillover, in: G. Garab (Ed.), *Photosynthesis: Mechanisms and Effects*, vol. 1, Kluwer Academic Publishers, Dordrecht, 1998, pp. 213–216.
- [24] L. Duysens, H. Sweers, Mechanism of the two photochemical reactions in algae as studied by means of fluorescence, in: J.S.o.P. Physiologists (Ed.), *Studies on Microalgae and Photosynthetic Bacteria*, University of Tokyo Press, Tokyo, 1963, pp. 353–372.
- [25] D. Fork, P. Mohanty, Fluorescence and other characteristics of blue-green algae (cyanobacteria), red algae, and cryptomonads, in: Govindjee, J. Amesz, D. Fork (Eds.), *Light Emission by Plants and Bacteria*, Academic Press, Orlando, FL, 1986, pp. 451–496.
- [26] U. Schreiber, C. Klughammer, C. Neubauer, Measuring P700 absorbance changes around 830 nm with a new type of pulse modulation system, *Z. Naturforsch.* 43C (1988) 686–698.
- [27] B. Genty, J. Briantias, N. Baker, The relationship between the quantum yield of photosynthetic electron transport and quenching of chlorophyll fluorescence, *Biochim. Biophys. Acta* 990 (1989) 87–92.
- [28] W. Bilger, O. Björkman, Role of the xanthophyll cycle in photoprotection elucidated by measurements of light-induced absorbance changes, fluorescence and photosynthesis in leaves of *Hedera canariensis*, *Photosynth. Res.* 25 (1990) 173–185.
- [29] R. Walters, P. Horton, Resolution of components of non-photochemical chlorophyll fluorescence quenching in barley leaves, *Photosynth. Res.* 27 (1991) 121–133.
- [30] L. Fridlyand, J. Backhausen, Homeostatic regulation upon changes of enzyme activities in the Calvin cycle as an example for general mechanisms of flux control. What can we expect from transgenic plants? *Photosynth. Res.* 6 (1999) 227–239.
- [31] G. Schansker, A. Srivastava, Govindjee, R. Strasser, Characterization of 820 nm transmission induction curves in pea leaves: kinetic separation between plastocyanin and P700 contributions, *Funct. Plant Biol.* 30 (2003) 1–10.
- [32] J. Munday Jr., Govindjee, Light-induced changes in the fluorescence yield of chlorophyll *a* in vivo: III. The dip and the peak in the fluorescence transient of *Chlorella pyrenoidosa*, *Biophys. J.* 9 (1969) 1–21.
- [33] V. Oja, H. Eichelmann, R. Peterson, B. Rasulov, A. Laisk, Deciphering the 820 nm signal: redox state of donor side and quantum yield of Photosystem I in leaves, *Photosynth. Res.* (2003) (in press).
- [34] C. Foyer, R. Furbank, J. Harbinson, P. Horton, The mechanisms contributing to photosynthetic control of electron transport by carbon assimilation in leaves, *Photosynth. Res.* 25 (1990) 83–100.
- [35] P. Joliot, A. Joliot, Cyclic electron transfer in plant leaf, *Proc. Natl. Acad. Sci. U. S. A.* 99 (2002) 10209–10214.
- [36] U. Heber, D. Walker, Concerning a dual function of coupled cyclic electron transport in leaves, *Plant Physiol.* 100 (1992) 1621–1626.
- [37] A. Laisk, H. Eichelmann, V. Oja, A. Eatherall, D. Walker, A mathematical model of the carbon metabolism in photosynthesis—difficulties in explaining oscillations by fructose 2,6-bisphosphate regulation, *Proc. R. Soc. Lond.*, B 237 (1989) 389–415.
- [38] A. Laisk, H. Eichelmann, Towards understanding oscillations: a mathematical model of the biochemistry of photosynthesis, *Philos. Trans. R. Soc. Lond.*, B 323 (1989) 369–384.
- [39] A. Laisk, Mathematical modelling of free-pool and channelled electron transport in photosynthesis: evidence for a functional supercomplex around Photosystem I, *Proc. R. Soc. Lond.*, B 251 (1993) 243–251.
- [40] M. Csete, J. Doyle, Reverse engineering of biological complexity, *Science* 295 (2002) 1664–1669.